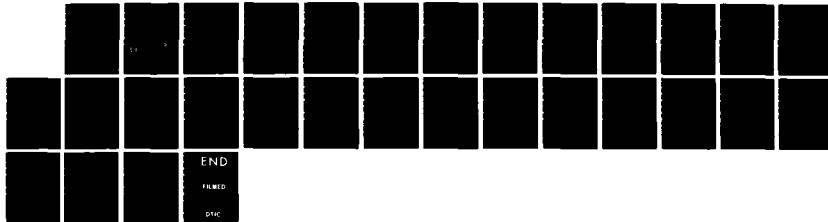


AD-A153 347 CYCLIC TORSION OF A CIRCULAR CYLINDER AND ITS RESIDUAL
STRESS DISTRIBUTION (U) ARMY ARMAMENT RESEARCH AND
DEVELOPMENT CENTER WATERVLIET NY L. H C WU ET AL.
UNCLASSIFIED FEB 85 ARLCB-TR-85006 SBI-AD-E440 274 1/1
F/G 20/11 NL



END
FILED
DTIC

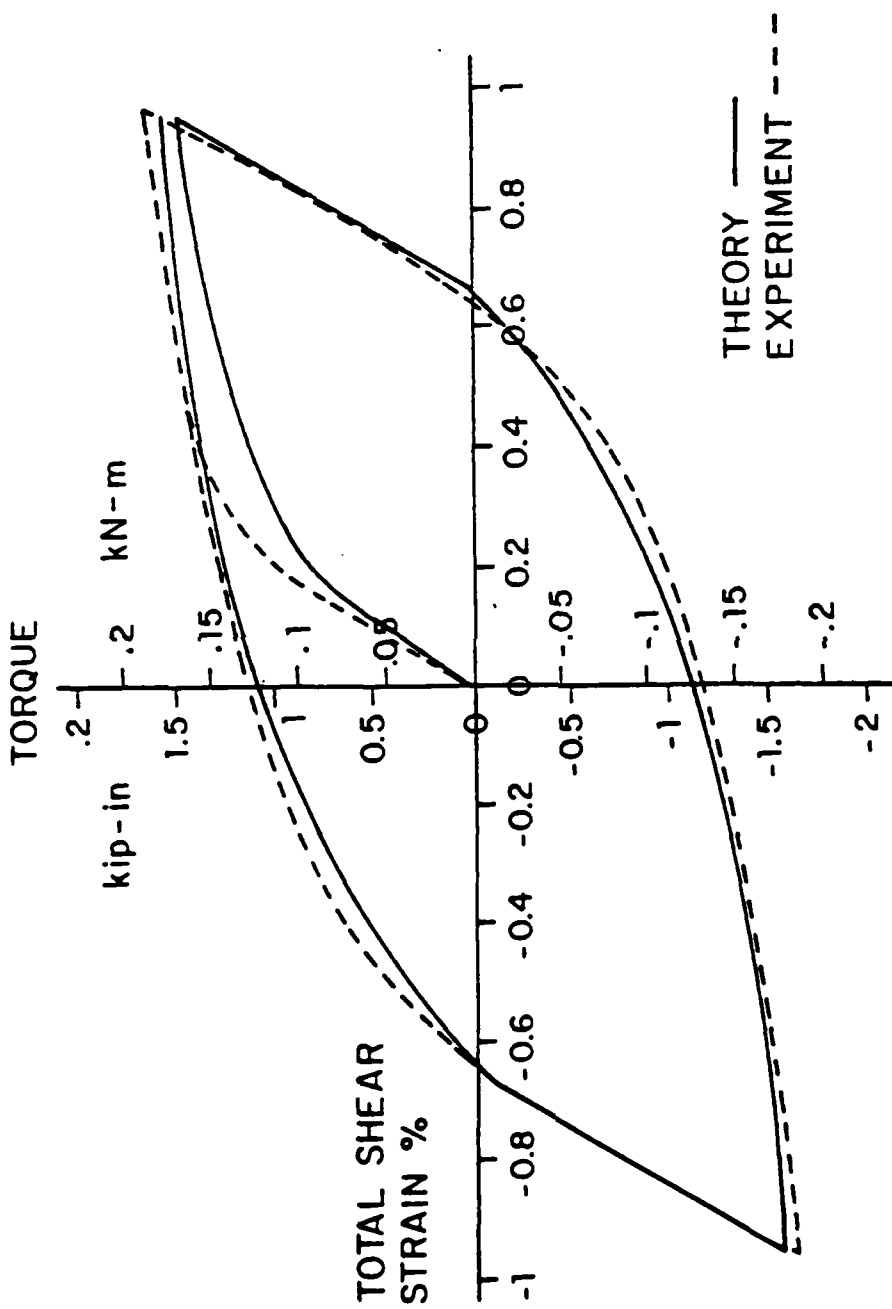


Figure 3. Torque-shear strain curves for solid circular cylinder.

AP-6 440274

2

AD

TECHNICAL REPORT ARLCB-TR-85006

CYCLIC TORSION OF A CIRCULAR CYLINDER AND ITS RESIDUAL STRESS DISTRIBUTION

AD-A153 347

HAN C. WU

M. R. ABOUTORABI

PETER C. T. CHEN

FEBRUARY 1985



US ARMY ARMAMENT RESEARCH AND DEVELOPMENT CENTER
LARGE CALIBER WEAPON SYSTEMS LABORATORY
BENET WEAPONS LABORATORY
WATERVLIET N.Y. 12189

DTIC FILE COPY

APPROVED FOR PUBLIC RELEASE; DISTRIBUTION UNLIMITED

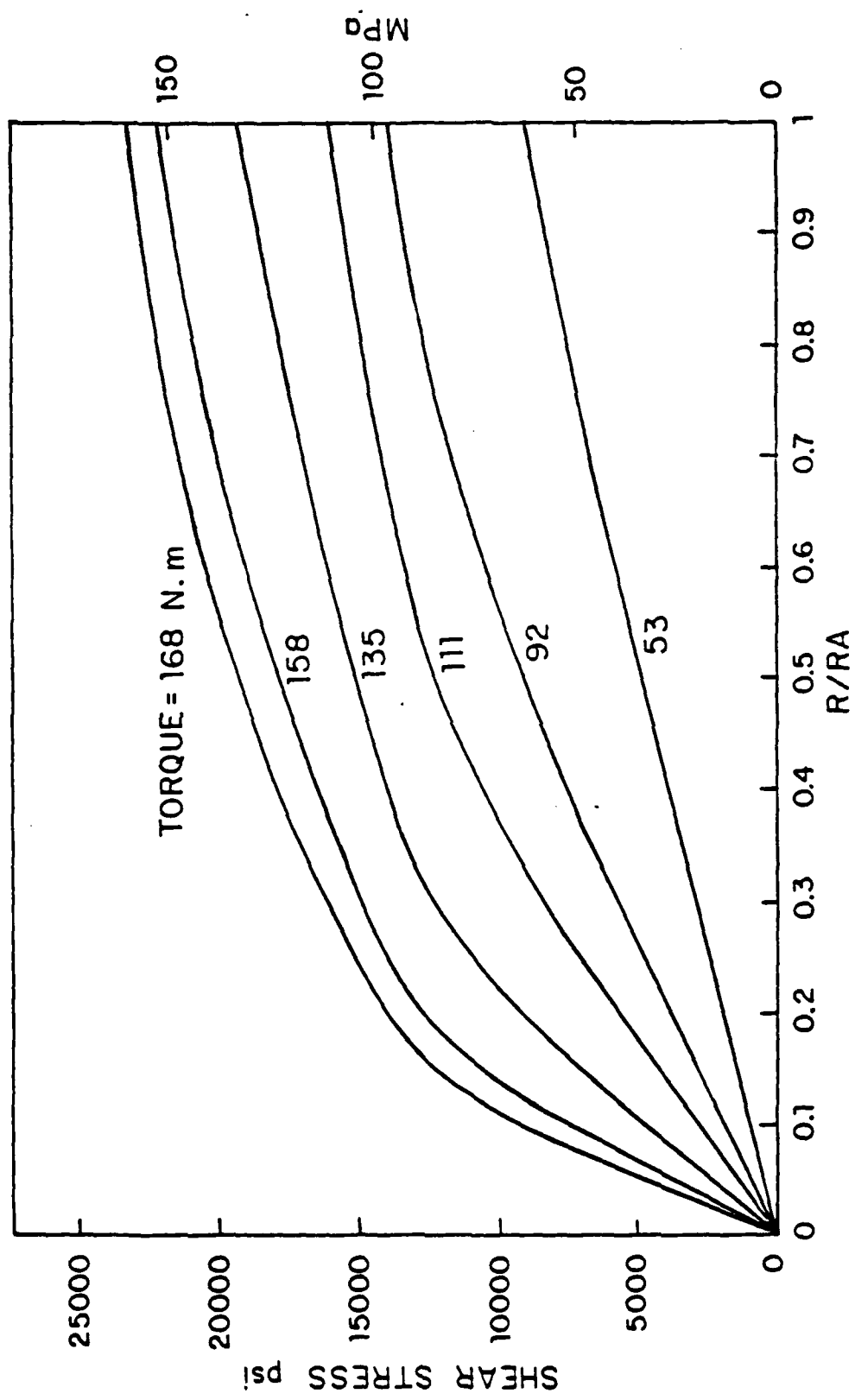


Figure 4. Stress distribution at different stages of first loading of solid cylinder.

DISCLAIMER

The findings in this report are not to be construed as an official Department of the Army position unless so designated by other authorized documents.

The use of trade name(s) and/or manufacture(s) does not constitute an official indorsement or approval.

DISPOSITION

Destroy this report when it is no longer needed. Do not return it to the originator.

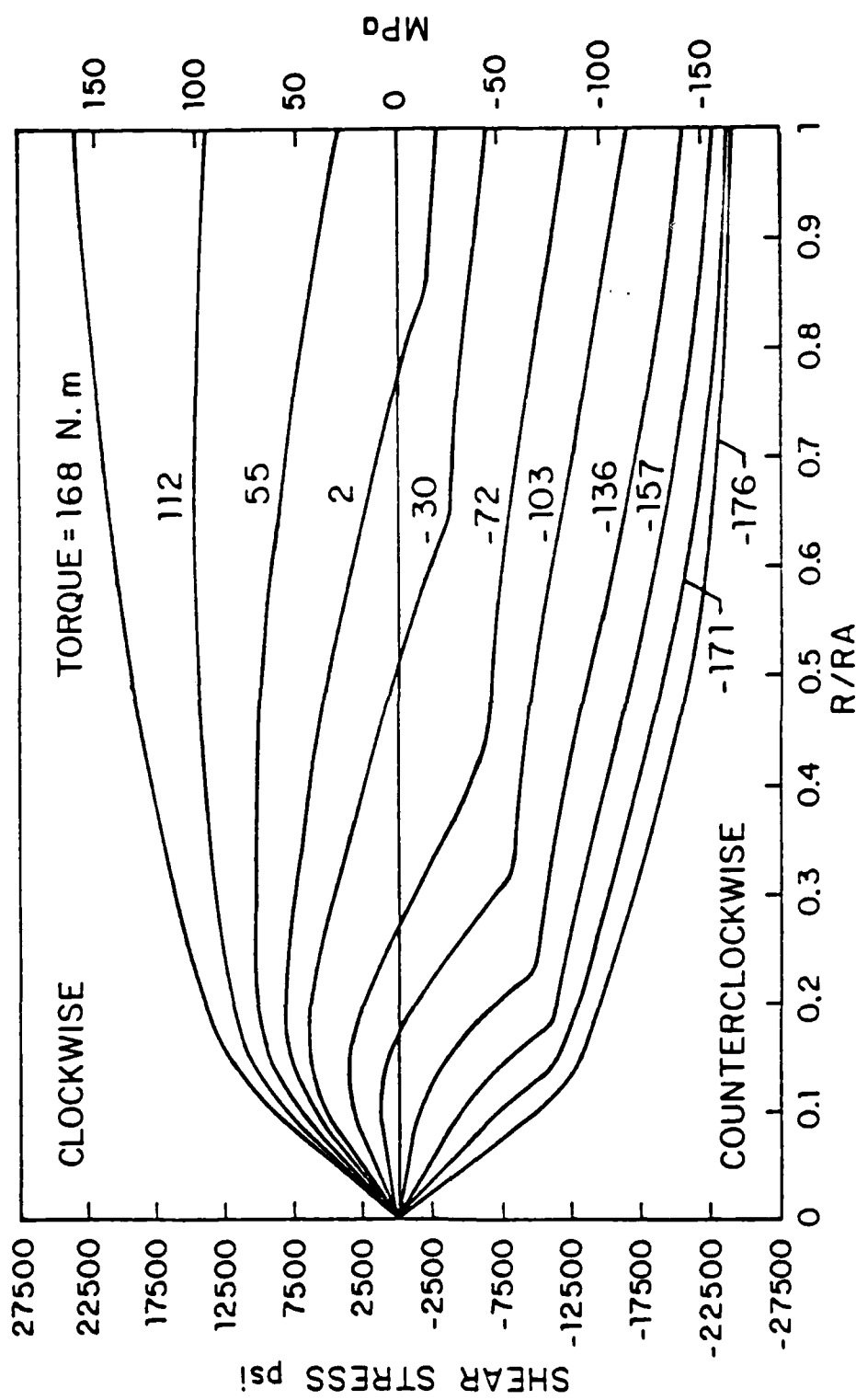


Figure 5. Stress distribution at different stages of first unloading of solid cylinder.

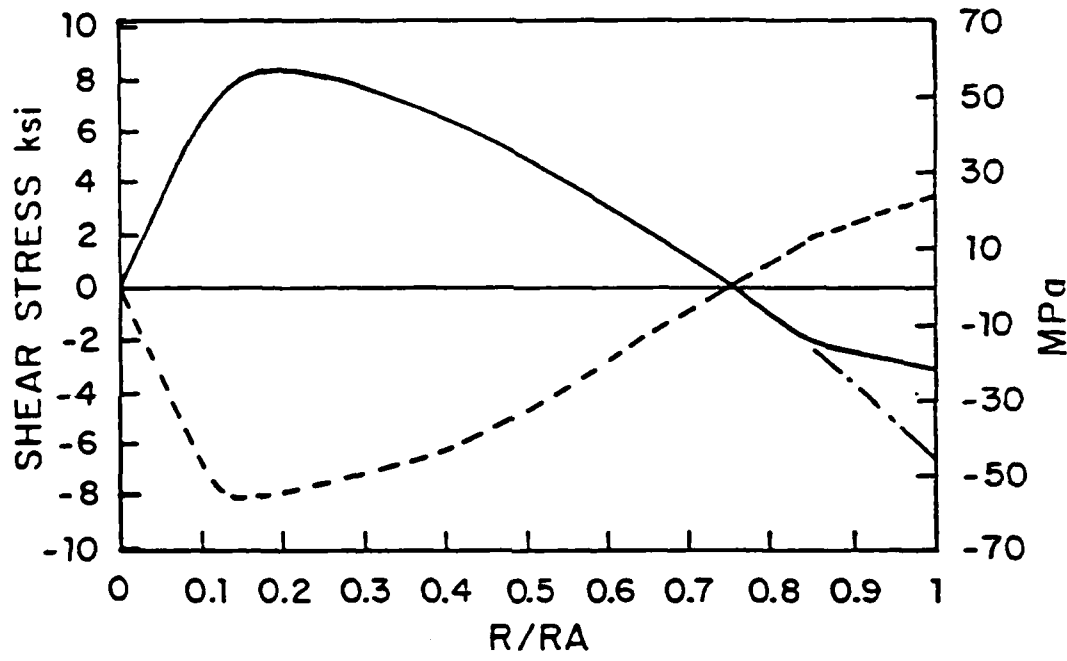


Figure 6. Residual stress distribution at zero torque.

REPORT DOCUMENTATION PAGE		READ INSTRUCTIONS BEFORE COMPLETING FORM
1. REPORT NUMBER ARLCB-TR-85006	2. GOVT ACCESSION NO. AD-A153347	3. RECIPIENT'S CATALOG NUMBER
4. TITLE (and Subtitle) CYCLIC TORSION OF A CIRCULAR CYLINDER AND ITS RESIDUAL STRESS DISTRIBUTION		5. TYPE OF REPORT & PERIOD COVERED Final
7. AUTHOR(s) Han C. Wu, M. R. Abutorabi, and Peter C. T. Chen (see reverse)		8. CONTRACT OR GRANT NUMBER(s)
9. PERFORMING ORGANIZATION NAME AND ADDRESS US Army Armament Research & Development Center Benet Weapons Laboratory, SMCAR-LCB-TL Watervliet, NY 12189-5000		10. PROGRAM ELEMENT, PROJECT, TASK AREA & WORK UNIT NUMBERS AMCMS No. 6111.02.H600.011 PRON No. 1A425M541A1A
11. CONTROLLING OFFICE NAME AND ADDRESS US Army Armament Research & Development Center Large Caliber Weapon Systems Laboratory Dover, NJ 07801-5001		12. REPORT DATE February 1985
14. MONITORING AGENCY NAME & ADDRESS(if different from Controlling Office)		13. NUMBER OF PAGES 22
15. SECURITY CLASS. (of this report) UNCLASSIFIED		
15a. DECLASSIFICATION/DOWNGRADING SCHEDULE		
16. DISTRIBUTION STATEMENT (of this Report) Approved for public release; distribution unlimited.		
17. DISTRIBUTION STATEMENT (of the abstract entered in Block 20, if different from Report)		
18. SUPPLEMENTARY NOTES To be published in <u>ASME Journal of Engineering Materials and Technology</u> .		
19. KEY WORDS (Continue on reverse side if necessary and identify by block number) Circular Cylinder Cyclic Torsion Residual Stresses Endochronic Theory of Plasticity		
20. ABSTRACT (Continue on reverse side if necessary and identify by block number) The endochronic theory of plasticity is applied to discuss the cyclic fully-reversed torsional loading of a solid bar with circular cross-section. Numerical techniques are employed to obtain the solution. The parameters of the constitutive equations are determined from the test data of thin-walled specimens. These parameters are then used without alteration to compute stress distributions within the solid specimen. Special attention is given to the (CONT'D ON REVERSE)		

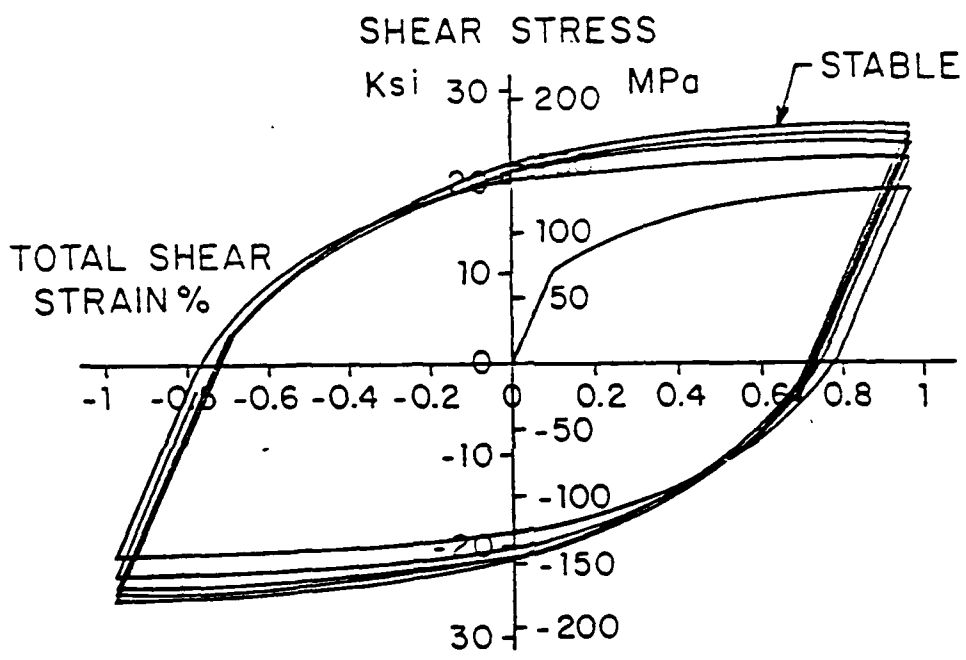


Figure 7. Theoretical shear stress-strain behavior of a hypothetical material.

7. AUTHORS (CONT'D)

Han C. Wu (Professor) and M. R. Aboutorabi (Graduate Student)
Department of Civil Engineering
University of Iowa
Iowa City, Iowa 52242

20. ABSTRACT (CONT'D)

residual stress distribution. It is shown that reasonable results are obtained. The relation of torque versus strain at the outermost fiber of the solid specimen provides an ultimate check of the theory as applied to this case.

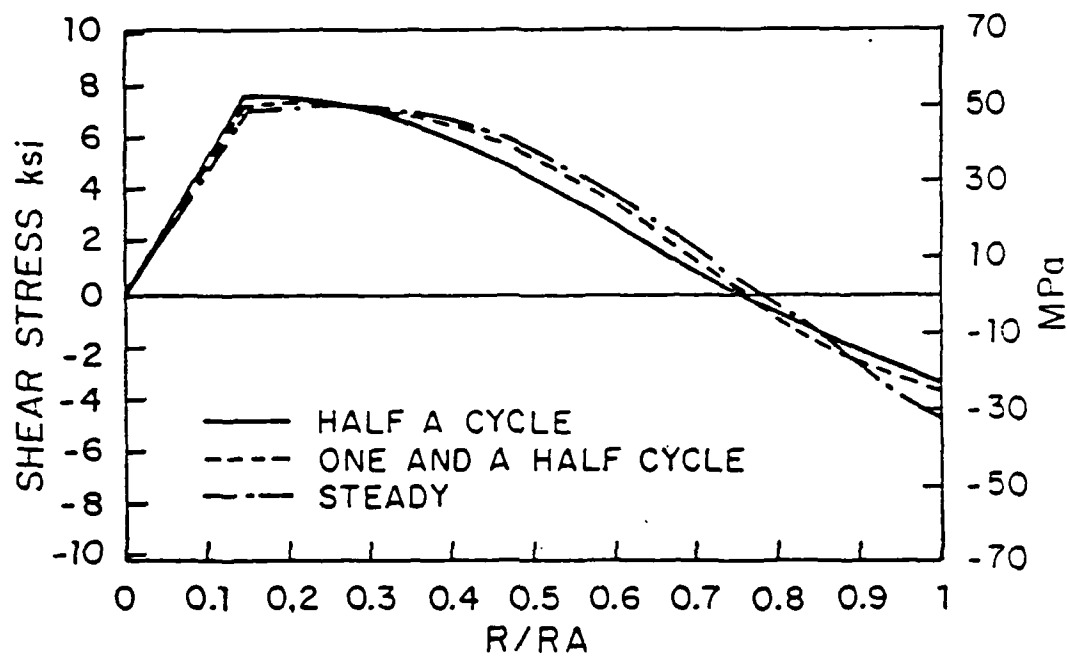


Figure 8. Residual stress distribution in a solid cylinder (hypothetical material) under cyclic torsion.

TABLE OF CONTENTS

	<u>Page</u>
INTRODUCTION	1
BRIEF SUMMARY OF ENDOCHRONIC THEORY	2
DESCRIPTION OF CYCLIC SHEAR RESPONSE	4
TORSION OF A CIRCULAR CYLINDER	6
COMPUTATION	8
RESULTS AND DISCUSSION	9
REFERENCES	12

LIST OF ILLUSTRATIONS

1. Specimen dimensions. 14
2. Shear stress-strain curves for thin-walled specimens. 15
3. Torque-shear strain curves for solid circular cylinder. 16
4. Stress distribution at different stages of first loading of solid cylinder. 17
5. Stress distribution at different stages of first unloading of solid cylinder. 18
6. Residual stress distribution at zero torque. 19
7. Theoretical shear stress-strain behavior of a hypothetical material. 20
8. Residual stress distribution in a solid cylinder (hypothetical material) under cyclic torsion. 21

Accession For	<input checked="" type="checkbox"/>
NTIS GRA&I	<input type="checkbox"/>
REFIC TAB	<input type="checkbox"/>
Declassify	<input type="checkbox"/>
Classification	<input type="checkbox"/>
Information	<input type="checkbox"/>
Availability	<input type="checkbox"/>
Comments	<input type="checkbox"/>

A



INTRODUCTION

Experimental observations indicate that when metallic materials are subjected to cyclic torsional loading, a hardening behavior similar to the case of uniaxial loading occurs. In a previous paper, Wu and Yip (ref 1) successfully applied the endochronic theory of plasticity to describe the cyclic hardening phenomenon under uniaxial loading. The present report applies this theory to the case of cyclic torsional loading of a thin-walled cylinder and a solid cylinder of circular cross-section, and it investigates the residual stress distribution.

The endochronic theory with plastic strain defined intrinsic time has previously been applied to describe several different experimentally observed phenomena (refs 1-6). We are now giving special attention to the prediction of residual stress by use of this theory.

Residual stresses are receiving increased attention by the engineering community. The primary goals are the reduction of cost of materials used in structures, the extension of the useful lifetime of existing structures, and the achievement of greater reliability of structural components through the understanding of residual stress distribution. This has led to much activity in the study of residual stress measurement methodologies, especially those which may be applied to nondestructive inspection. However, analytical investigation is also important so that residual stress fields in test specimens and engineering components may be determined. This information is particularly useful in the engineering design. In fact, by knowing the residual stress distribution, its beneficial effects may be exploited.

References are listed at the end of this report.

TECHNICAL REPORT EXTERNAL DISTRIBUTION LIST

<u>NO. OF COPIES</u>	<u>NO. OF COPIES</u>		
ASST SEC OF THE ARMY RESEARCH & DEVELOPMENT ATTN: DEP FOR SCI & TECH THE PENTAGON WASHINGTON, D.C. 20315	1	COMMANDER US ARMY AMCCOM ATTN: SMCAR-ESP-L ROCK ISLAND, IL 61299	1
COMMANDER DEFENSE TECHNICAL INFO CENTER ATTN: DTIC-DDA CAMERON STATION ALEXANDRIA, VA 22314	12	COMMANDER ROCK ISLAND ARSENAL ATTN: SMCR-ENM (MAT SCI DIV) ROCK ISLAND, IL 61299	1
COMMANDER US ARMY MAT DEV & READ COMD ATTN: DRCDE-SG 5001 EISENHOWER AVE ALEXANDRIA, VA 22333	1	DIRECTOR US ARMY INDUSTRIAL BASE ENG ACTV ATTN: DRXIB-M ROCK ISLAND, IL 61299	1
COMMANDER ARMAMENT RES & DEV CTR US ARMY AMCCOM ATTN: SMCAR-LC	1	COMMANDER US ARMY TANK-AUTMV R&D COMD ATTN: TECH LIB - DRSTA-TSL WARREN, MI 48090	1
SMCAR-LCE	1	COMMANDER	
SMCAR-LCM (BLDG 321)	1	US ARMY TANK-AUTMV COMD	
SMCAR-LCS	1	ATTN: DRSTA-RC	
SMCAR-LCU	1	WARREN, MI 48090	
SMCAR-LCW	1	COMMANDER	
SMCAR-SCM-O (PLASTICS TECH EVAL CTR, BLDG. 351N)	1	US MILITARY ACADEMY	
SMCAR-TSS (STINFO)	2	ATTN: CHMN, MECH ENGR DEPT	
DOVER, NJ 07801		WEST POINT, NY 10996	1
DIRECTOR BALLISTICS RESEARCH LABORATORY ATTN: AMXBR-TSB-S (STINFO) ABERDEEN PROVING GROUND, MD 21005	1	US ARMY MISSILE COMD REDSTONE SCIENTIFIC INFO CTR	
MATERIEL SYSTEMS ANALYSIS ACTV ATTN: DRXSY-MP ABERDEEN PROVING GROUND, MD 21005	1	ATTN: DOCUMENTS SECT, BLDG. 4484 REDSTONE ARSENAL, AL 35898	2
		COMMANDER	
		US ARMY FGN SCIENCE & TECH CTR	
		ATTN: DRXST-SD	
		220 7TH STREET, N.E.	
		CHARLOTTESVILLE, VA 22901	

NOTE: PLEASE NOTIFY COMMANDER, ARMAMENT RESEARCH AND DEVELOPMENT CENTER,
US ARMY AMCCOM, ATTN: BENET WEAPONS LABORATORY, SMCAR-LCB-TL,
WATERVLIET, NY 12189, OF ANY ADDRESS CHANGES.

$$d\Omega_{ij} = de_{ij} - k_1 \frac{ds_{ij}}{2\mu_0} \quad (2)$$

where Ω_{ij} is a strain-like tensor, e_{ij} and s_{ij} are deviatoric strain and stress tensors respectively, k_1 is a positive constant such that $0 < k_1 < 1$, and μ_0 is shear modulus.

The general constitutive equation for shear response of a material with an elastic hydrostatic response and no coupling between deviatoric and hydrostatic behavior is:

$$s_{ij} = 2 \int_0^z \mu(z-z') \frac{de_{ij}}{dz'} dz' \quad (3)$$

where z is an intrinsic time which is related to ζ by the following time scale:

$$\frac{d\zeta}{dz} = f(\zeta) \quad (4)$$

It has been shown in Reference 12 that $f(\zeta)$ describes isotropic hardening and is therefore termed the hardening function.

Define

$$\mu(z) = \mu_0 G(z) \quad (5)$$

where $G(0) = 1$ indicates initially elastic response. Using the Laplace transform technique (for details see Reference 12), Eq. (3) becomes

$$s_{ij} = 2\mu_0 \int_0^z \rho(z-z') \frac{d\Omega_{ij}}{dz'} dz' \quad (6)$$

in which, for the case of $k_1 = 1$,

$$\rho(z) = \rho_0 \delta(z) + \rho_1(z) \quad (7)$$

where $\rho_1(z)$ is composed of a finite sum of exponential terms, ρ_0 is constant, and $\delta(z)$ is the Dirac delta function. A general constitutive equation in

TECHNICAL REPORT EXTERNAL DISTRIBUTION LIST (CONT'D)

<u>NO. OF COPIES</u>	<u>NO. OF COPIES</u>		
COMMANDER US ARMY MATERIALS & MECHANICS RESEARCH CENTER ATTN: TECH LIB - DRXMR-PL WATERTOWN, MA 01272	2	DIRECTOR US NAVAL RESEARCH LAB ATTN: DIR, MECH DIV CODE 26-27, (DOC LIB) WASHINGTON, D.C. 20375	1
COMMANDER US ARMY RESEARCH OFFICE ATTN: CHIEF, IPO P.O. BOX 12211 RESEARCH TRIANGLE PARK, NC 27709	1	COMMANDER AIR FORCE ARMAMENT LABORATORY ATTN: AFATL/DLJ AFATL/DLJG EGLIN AFB, FL 32542	1
COMMANDER US ARMY HARRY DIAMOND LAB ATTN: TECH LIB 2800 POWDER MILL ROAD ADELPHIA, MD 20783	1	METALS & CERAMICS INFO CTR BATTELLE COLUMBUS LAB 505 KING AVENUE COLUMBUS, OH 43201	1
COMMANDER NAVAL SURFACE WEAPONS CTR ATTN: TECHNICAL LIBRARY CODE X212 DAHLGREN, VA 22448	1		

NOTE: PLEASE NOTIFY COMMANDER, ARMAMENT RESEARCH AND DEVELOPMENT CENTER,
US ARMY AMCCOM, ATTN: BENET WEAPONS LABORATORY, SMCAR-LCB-TL,
WATERVLIET, NY 12189, OF ANY ADDRESS CHANGES.

terms of initial yield stress s_y and plastic strain $\Omega_{ij}(k_1 = 1)$ can be obtained as

$$s_{ij} = s_y \frac{d\Omega_{ij}}{dz} + 2\mu_0 \int_0^z \rho_1(z-z') \frac{d\Omega_{ij}}{dz'} dz' \quad (8)$$

by substituting Eq. (7) into Eq. (6) and defining $s_y = 2\mu_0\rho_0$. Note that at $z = 0$:

$$s_{ij} = s_y \left. \frac{d\Omega_{ij}}{dz} \right|_{z=0} \quad (9)$$

Also from Eq. (2), the condition $\Omega_{ij} = 0$ gives the relation,

$$s_{ij} = 2\mu_0 e_{ij} \quad (10)$$

Equation (10) merely attests to the fact that while $z = 0$, the deformation process is reversible and therefore the deviatoric stress response is elastic.

DESCRIPTION OF CYCLIC SHEAR RESPONSE

For pure shear deformation with $\rho_1(z)$ represented by one exponential term, one has

$$d\Omega = dn - \frac{d\tau}{2\mu_0} \quad (11a)$$

and

$$2\mu_0\rho_1(z) = 2\mu_1 e^{-\alpha z} \quad (11b)$$

where n is total shear strain and Ω is plastic shear strain. Equation (8) yields

$$\tau = \tau_y \frac{d\Omega}{dz} + 2\mu_1 \int_0^z e^{-\alpha(z-z')} \frac{d\Omega}{dz'} dz' \quad (12)$$

with

$$\frac{d\zeta}{dz} = f(z) \text{ and } d\zeta = |d\Omega| \quad (13)$$

END

FILMED

5-85

DTIC

and τ_y is the shear yield stress. Using Eqs. (12) and (13) and a suitable function f , the governing equations for torsional test of a thin-walled tube during loading, unloading, and reloading can be derived. The initially elastic unloading (reloading) response and following Bauschinger effect will be governed by the material property itself, provided that the intrinsic time measurement is correct.

If the first unloading of stress-strain curve begins when intrinsic time measure ζ reaches ζ^* , the positive property of ζ requires Eq. (13) to be

$$d\zeta = -d\Omega \quad (14)$$

during unloading. Define ζ_-^* and ζ_+^* as loading and unloading measures around the neighborhood of ζ^* in ζ space. Then Eq. (12) leads to

$$\tau^- = \tau_y \frac{d\zeta}{dz} \Big|_{\zeta_-^*} + 2\mu_1 \int_0^{z^*} e^{-\alpha(z-z')} \frac{d\Omega}{dz'} dz' \quad (15)$$

$$\tau^+ = -\tau_y \frac{d\zeta}{dz} \Big|_{\zeta_+^*} + 2\mu_1 \int_0^{z^*} e^{-\alpha(z-z')} \frac{d\Omega}{dz'} dz' \quad (16)$$

where τ^- and τ^+ are stress states nearby ζ^* at loading and unloading processes, respectively. In the limit, when $\zeta_-^* \rightarrow \zeta^*$ and $\zeta_+^* \rightarrow \zeta^*$,

$$\tau^- - \tau^+ = 2\tau_y \frac{d\zeta}{dz} \Big|_{\zeta^*} \quad (17)$$

Therefore, the shear stress is discontinuous with a discontinuity of magnitude

$$\Delta\tau = 2\tau_y \frac{d\zeta}{dz} \Big|_{\zeta^*} \quad (18)$$

in the initially elastic unloading region. If the consequent loading reversals take place at ζ^{**} , ζ^{***} , ..., then there is an elastic change of

magnitude

$$\Delta\tau = 2\tau_y \frac{d\zeta}{dz} \Big|_{\zeta^{**}, \zeta^{***}, \dots} \quad (19)$$

in the shear stress at each point of load reversal. During these elastic responses, the values of ζ and z remain unchanged.

During the elastic response, $d\zeta$ is zero and the constitutive equation is simply

$$d\tau = 2\mu_0 dn \quad (20)$$

Once the change in stress is larger than $\tau^- - \tau^+$, then the material behavior is governed by Eq. (12).

TORSION OF A CIRCULAR CYLINDER

In laboratory experiments on torsion of solid bars, the recorded data are usually the strain at the outer fiber and the amount of externally applied torque. In order to describe these experimental results, the shear constitutive equation established in the previous section and based on a thin-walled tubular specimen should be applied together with the equations discussed in this section.

The external torque for a solid bar with a circular cross-section is given as:

$$T_s = 2\pi \int_0^{r_a} \tau r^2 dr \quad (21)$$

where τ is current shear stress state corresponding to location r , and r_a is the radius of cross-section. The torque can be approximated by discretizing the circular cross-section into a finite number of concentric circular rings and assuming τ to be constant over each ring. Thus

$$T_s = 2\pi \sum_{i=1}^n \tau_i r_i^2 \Delta r_i \quad (22)$$

Now Eqs. (12) and (13) along with Eq. (11a) can be solved to yield τ_i at each fiber, if the value of η_i (shear strain) at that fiber, specified by radius r_i , is known. Geometrical considerations show that radial lines have to remain straight after deformation. Thus, one concludes that

$$\eta_i = \frac{r_i}{r_a} \eta_a \quad (23)$$

where η_a is the strain at the outermost fiber.

Recall that there is a yield stress introduced in Eq. (8) when $k_1 = 1$ and $\zeta = 0$. Hence, an elastic core always exists during deformation whose radius r_e is easily computed as

$$r_e = \frac{\tau_y}{2\mu_0} \frac{r_a}{\eta_a} \quad (24)$$

If the experiment is strain-controlled with strain at r_a varying between $-\eta_a$ and $+\eta_a$, and with η_a in the plastic range, then the elastic core radius remains fixed during all stages of loading after the first load reversal.

Now that η_i is known, the value of shear stress at each fiber τ_i can be evaluated and used in Eq. (22). Note that at the points of load reversal, for the fibers in the plastically deformed region, there exists an elastic range governed by Eq. (19). This discrete type formulation of torque has the advantage of being capable of describing the transient and residual stresses in the bar as well.

COMPUTATION

The governing equations are Eqs. (11a), (12), (13), (22), and (23) which are summarized below:

$$d\Omega = dn - \frac{d\tau}{2\mu_0} \quad (11a)$$

$$\tau = \tau_y \frac{d\Omega}{dz} + 2\mu_1 \int_0^z e^{-\alpha(z-z')} \frac{d\Omega}{dz'} dz' \quad (12)$$

$$\frac{d\zeta}{dz} = f(z) \text{ and } d\zeta = |d\Omega| \quad (13)$$

$$T_s = 2\pi \sum_{i=1}^n \tau_i r_i^2 \Delta r_i \quad (22)$$

$$n_i = \frac{r_i}{r_a} n_a \quad (23)$$

Since the analytical solution of these equations is quite involved, and in particular requires different treatment and derivation for different hardening functions $f(z)$, a numerical scheme has been developed to solve the above equations. Since the relationship between ζ , the independent variable, and n , the controlled variable is indirect, iterative techniques are an integral part of this program.

In order to ascertain the degree of accuracy of numerical methods, a hypothetical case was assumed. Namely, the field equations were solved analytically using $f(z) = \exp(\beta z)$, and the results were compared with those obtained numerically. The difference between the two is so small that using numerical techniques does not introduce any significant amount of error.

RESULTS AND DISCUSSION

Once the accuracy of the computer program was established, it was used to predict the results of experiments performed on annealed AISI 4142 steel. Figure 1 shows the dimensions of the tubular specimens, and these are also the dimensions (without ID) of the solid specimens. The experimental results of cyclic torsion tests conducted by the Plasticity Research Laboratory at The University of Iowa are presented along with the theoretical predictions in Figures 2 and 3. This material does not show any appreciable amount of cyclic hardening.

The most important factor in theoretical predictions is the choice of the hardening function $f(z)$. In this computation, the form

$$\frac{d\zeta}{dz} = C - (C-1)e^{-\beta z} \quad (25)$$

has been used because of its simplicity and its proven usefulness in case of cyclic loading (ref 1).

Following accepted procedures, the shear stress-strain curve for the material was obtained from thin-walled tubular specimens. Then from this data, the values of the material constants were determined to be: $\alpha = 1100$, $\beta = 30,000$, $C = 1.9$, $\mu_0 = 1 \times 10^7$ psi (6.89×10^4 MPa), $\mu_1 = 3.6 \times 10^6$ psi (24.804×10^3 MPa), $\tau_y = 6,500$ psi (44.79 MPa). As can be seen from Figure 2 this set of constants predicts the experimental results reasonably well. The same set of constants was then used to predict the results for a solid bar test. As evidenced in Figure 3, theoretical and experimental results are in reasonable agreement.

As a consequence of the computational process the distribution of stress in the cross-section was evaluated. Such distribution at different magnitudes of torque during the first loading half-cycle is presented in Figure 4. Notice that the outer fiber is the first one to yield; subsequently as more torque is applied, the radius of the elastic inner core gets smaller.

Figure 5 presents the distribution of the shear stress in the bar at different stages of the first unloading. The flat portion in the lower curves corresponds to the fibers which have surpassed this initial elastic unloading and started plastic unloading. An interesting observation can be made here; when the amount of reversed torque gets larger, the size of the plastically deformed region, i.e., the flat portion, gets bigger as well, but for each individual fiber the developed plastic stress does not increase accordingly. Rather, the applied torque is compensated for by elastic relief of shear stress in the internal fibers. The radius of the elastic core has been found to be $r_e/r_a = 0.0913$ for this computation.

Shown in Figure 6 are the residual shear stress distributions during first unloading (the solid curve) and first reloading (the dashed curve) when the applied torque is equal to zero. The solid curve is the favorable one if the applied torque during service is in the same direction as the initial loading. However, if the applied torque during service is in the reversed direction, then neither advantageous nor detrimental effects can be claimed as is shown by Figure 5. It is seen that the residual stress distribution of Figure 6 agrees with that proposed by Swift (ref 11) and that the residual shear stress at the surface of the cylinder is smaller than that obtained by neglecting the Bauschinger effect in the calculation.

For purposes of investigating the implications of the model developed here, a hypothetical material with appreciable cyclic hardening behavior was studied. The shear stress-strain behavior of such material under fully-reversed torsional loading is presented in Figure 7. The material constants for this material were determined as: $\alpha = 1,000$, $\beta = 50$, $C = 1.5$, $u_0 = 1 \times 10^7$ psi (6.89×10^4 MPa), $u_1 = 4 \times 10^6$ psi (27.56×10^3 MPa), and $\tau_y = 10,000$ psi (68.9 MPa). A steady loop is established after a few cycles.

Figure 8 presents the residual stress distribution at zero applied torque for each cycle up to and including the steady loop. It is seen that the residual stress distribution does not change very much with respect to cyclic torsion. The small increase in the residual stress incurred at the exterior fiber at steady state is on the safe side when service load is applied.

REFERENCES

1. Wu, H. C. and Yip, M. C., "Endochronic Description of Cyclic Hardening Behavior for Metallic Materials," ASME J. of Eng. Materials and Technology, Vol. 103, July 1981, pp. 212-217.
2. Wu, H. C. and Yip, M. C., "Strain Rate and Strain Rate History Effects on the Dynamic Behavior of Metallic Materials," Int. J. Solids Structures, Vol. 16, 1980, pp. 515-536.
3. Lin, H. C. and Wu, H. C., "On the Rate-Dependent Endochronic Theory of Viscoplasticity and Its Application to Plastic-Wave Propagation," Int. J. Solids Structures, Vol. 19, 1983, pp. 587-599.
4. Wu, H. C. and Yang, R. J., "Application of the Improved Endochronic Theory of Plasticity to Loading with Multi-Axial Strain-Path," Int. J. Non-Linear Mechanics, Vol. 18, 1983, pp. 395-408.
5. Wu, H. C. and Yang, C. C., "Investigation of the One-Dimensional Endochronic Constitutive Equation for Metals by the Rivlin Test," ASME J. of Eng. Materials and Technology (in press).
6. Wu, H. C. and Yao, J. C., "Analysis of Stress Response to Various Strain-Paths in Axial Torsional Deformation of Metals," ASME J. Eng. Materials and Technology (in press).
7. Milligan, R. V., Koo, W. H., and Davidson, T. E., "The Bauschinger Effect in High-Strength Steel," ASME J. Basic Engng., Vol. 88, 1966, pp. 480-487.
8. Sidebottom, O. M. and Chang, C., "Influence of the Bauschinger Effect on Inelastic Bending of Beams," Proceedings First U.S. Cong. Appl. Mech., 1951, pp. 631-639.

9. Franklin, G. J. and Morrison, J. L. M., "Autofrettage of Cylinders: Prediction of Pressure/External Expansion Curves and Calculation of Residual Stresses," Proc. Instn. Mech. Engrs., Vol. 174, 1961, pp. 947-974.
10. Fuchs, H. O. and Mattson, R. L., "Measurement of Residual Stresses in Torsion-Bar Springs," Proceedings S.E.S.A., Vol. 4, 1946, pp. 64-73.
11. Swift, W. A. C., "On the Measurement of Residual Shear Stress in Scrapped Torsion Bars," J. Strain Analysis, Vol. 13, 1978, pp. 157-163.
12. Valanis, K. C., "Fundamental Consequences of a New Intrinsic Time Measure - Plasticity as a Limit of the Endochronic Theory," Archives of Mechanics, Vol. 32, 1980, pp. 171-191.

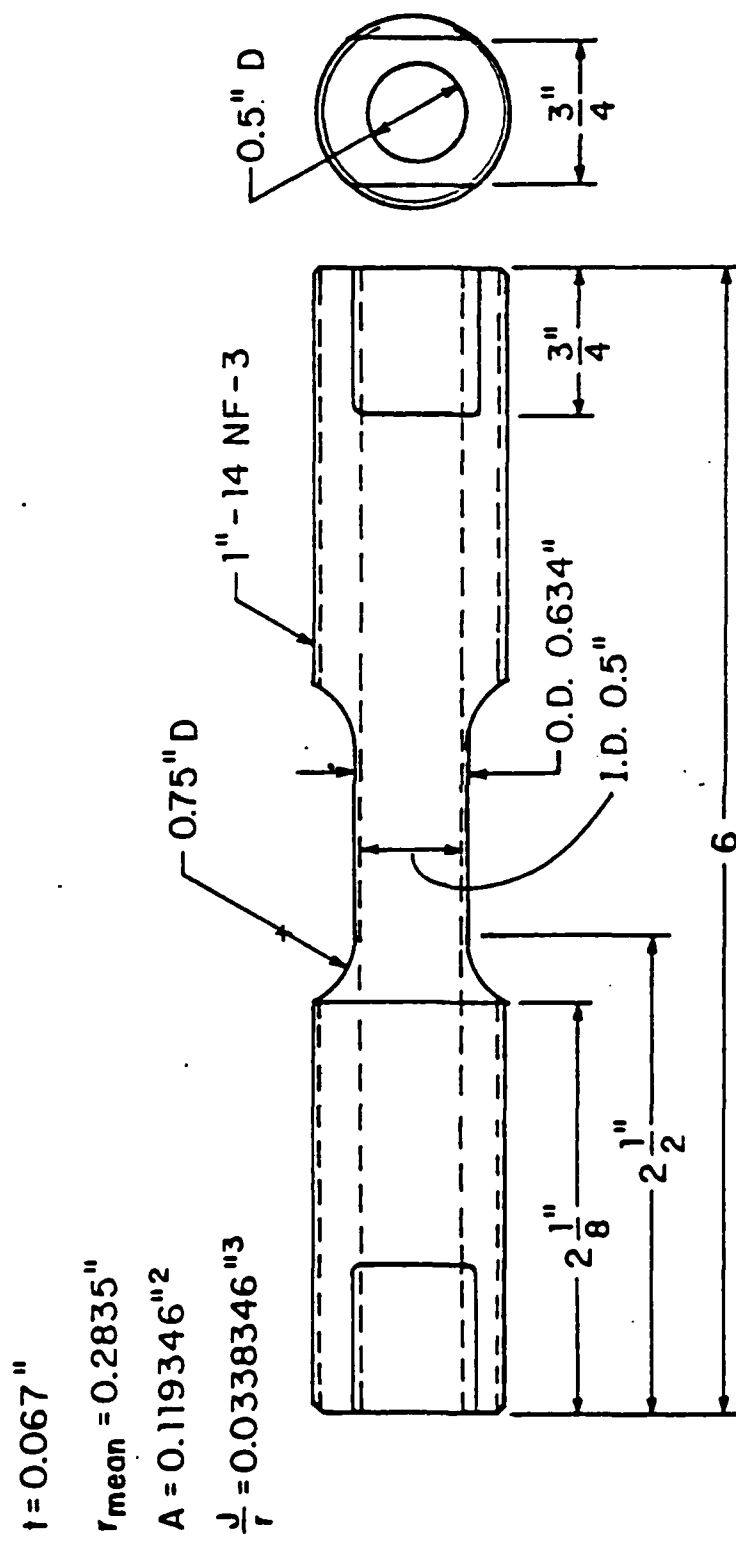


Figure 1. Specimen dimensions.

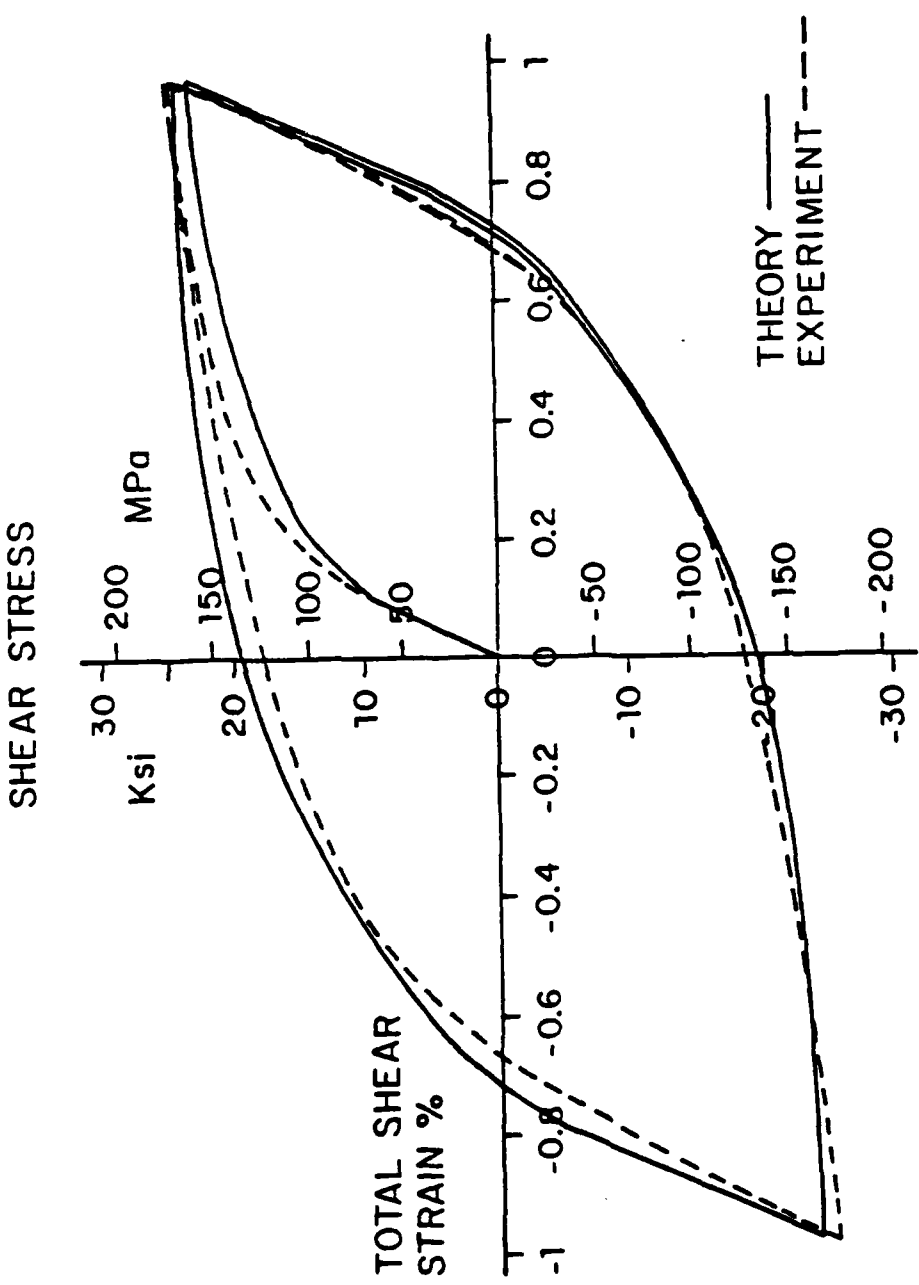


Figure 2. Shear stress-strain curves for thin-walled specimens.

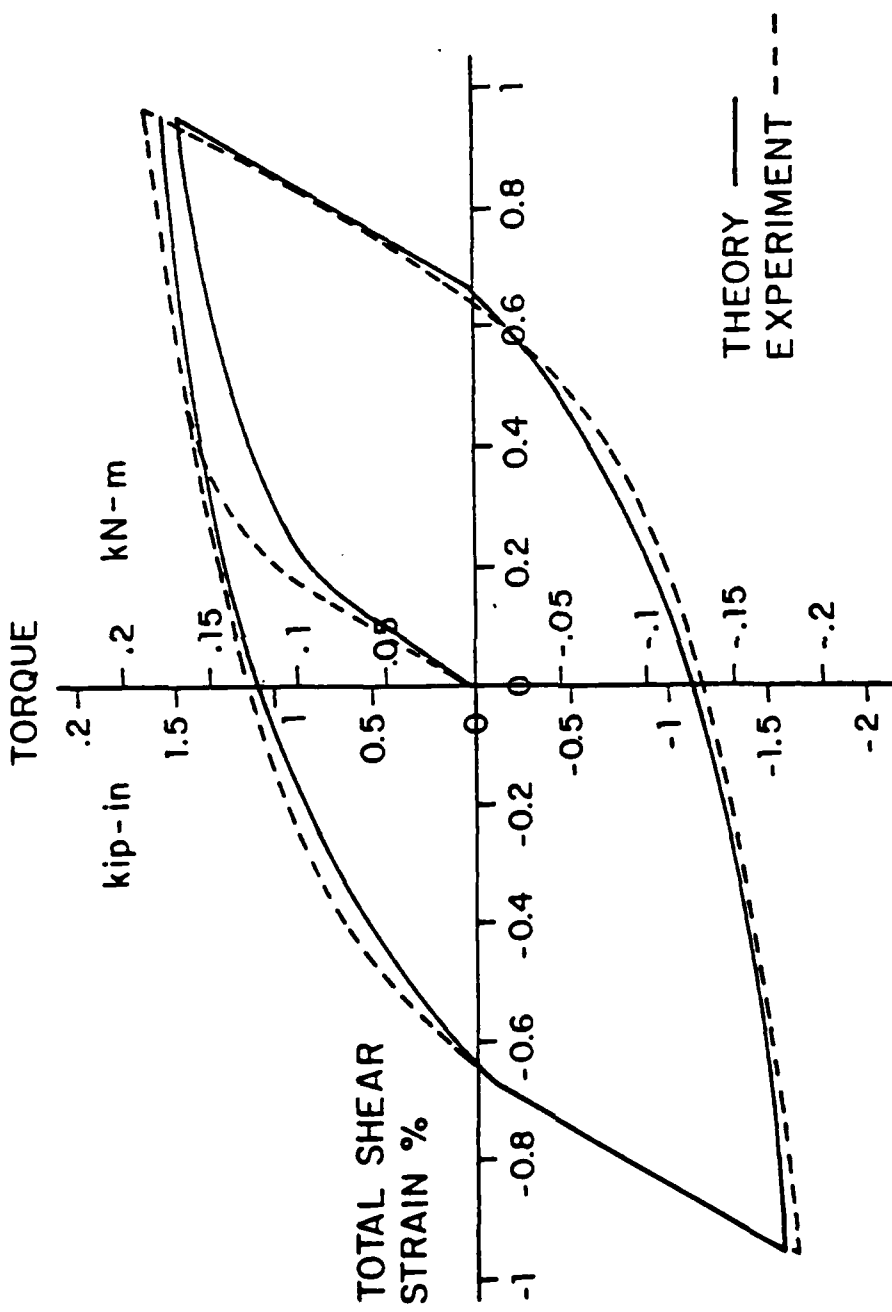


Figure 3. Torque-shear strain curves for solid circular cylinder.

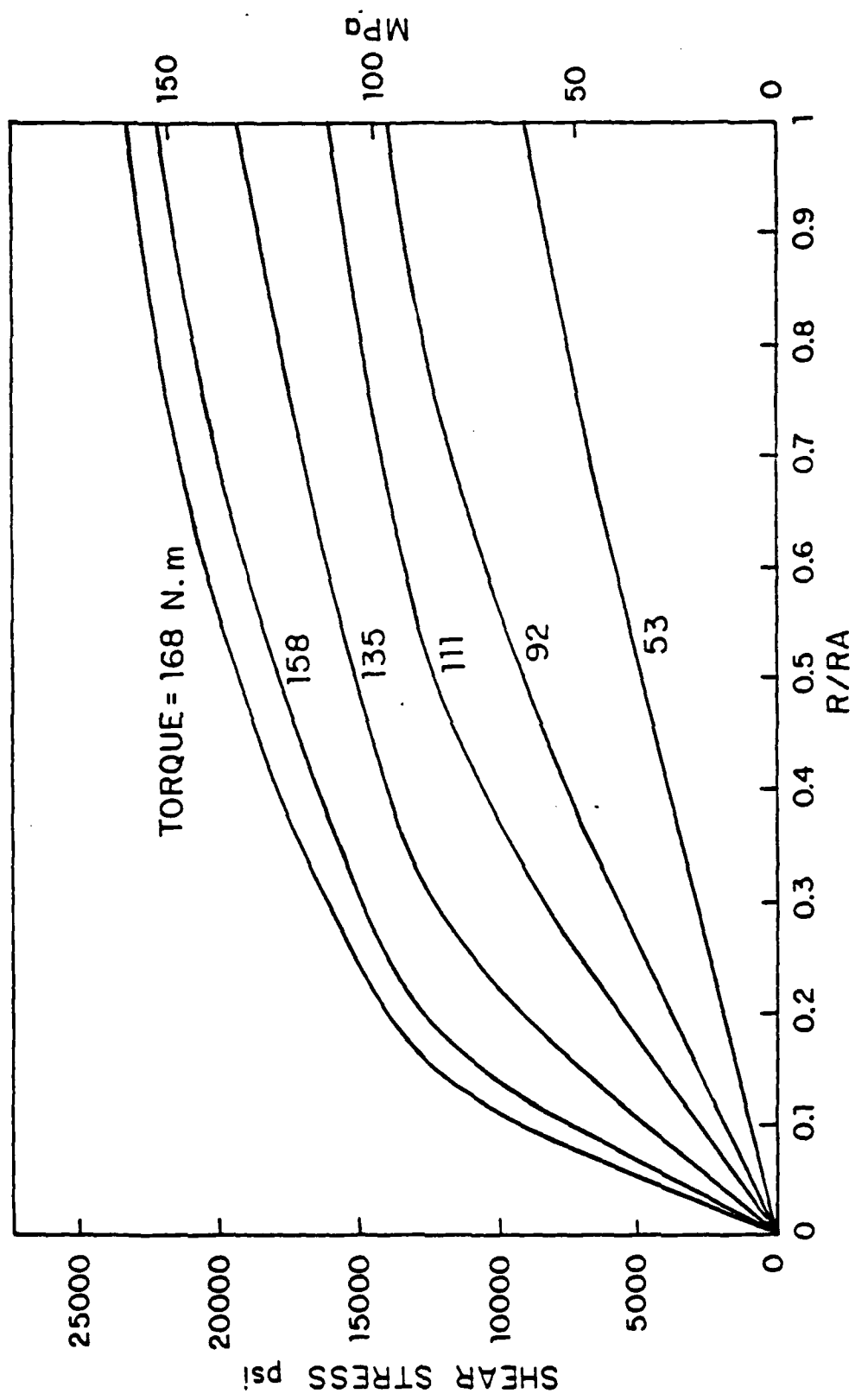


Figure 4. Stress distribution at different stages of first loading of solid cylinder.

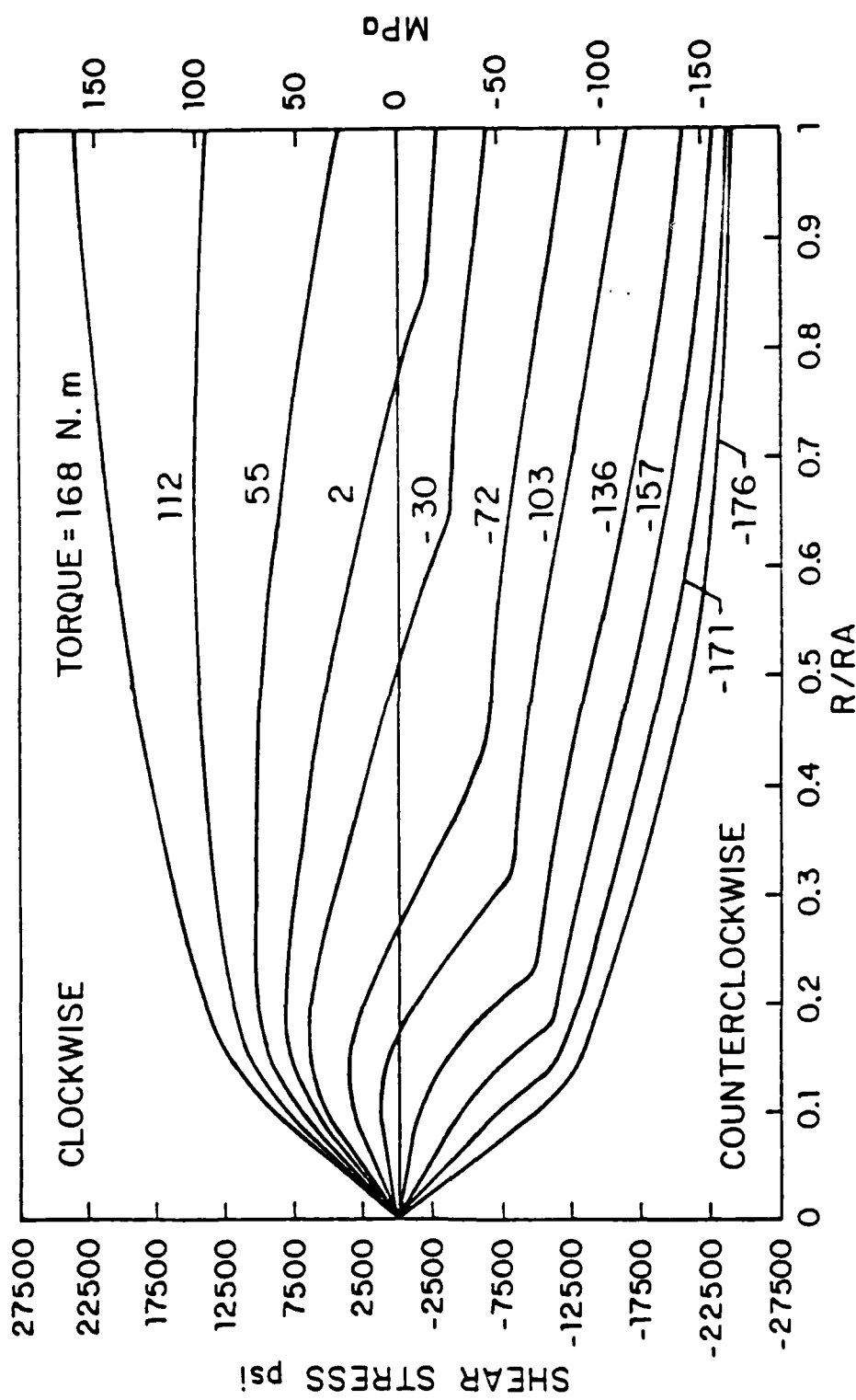


Figure 5. Stress distribution at different stages of first unloading of solid cylinder.

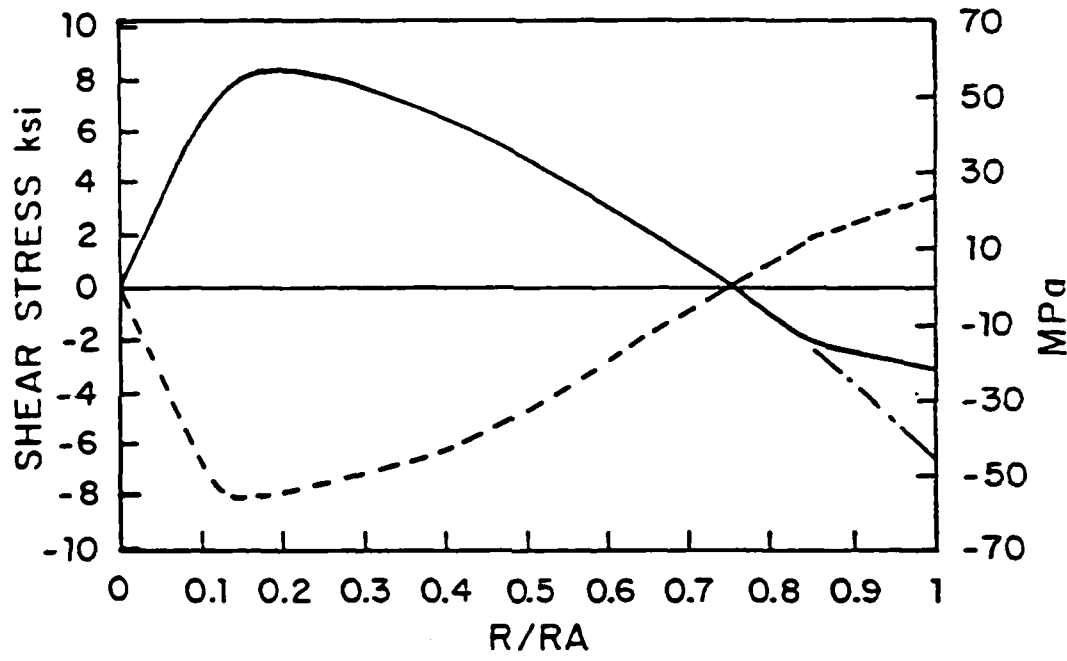


Figure 6. Residual stress distribution at zero torque.

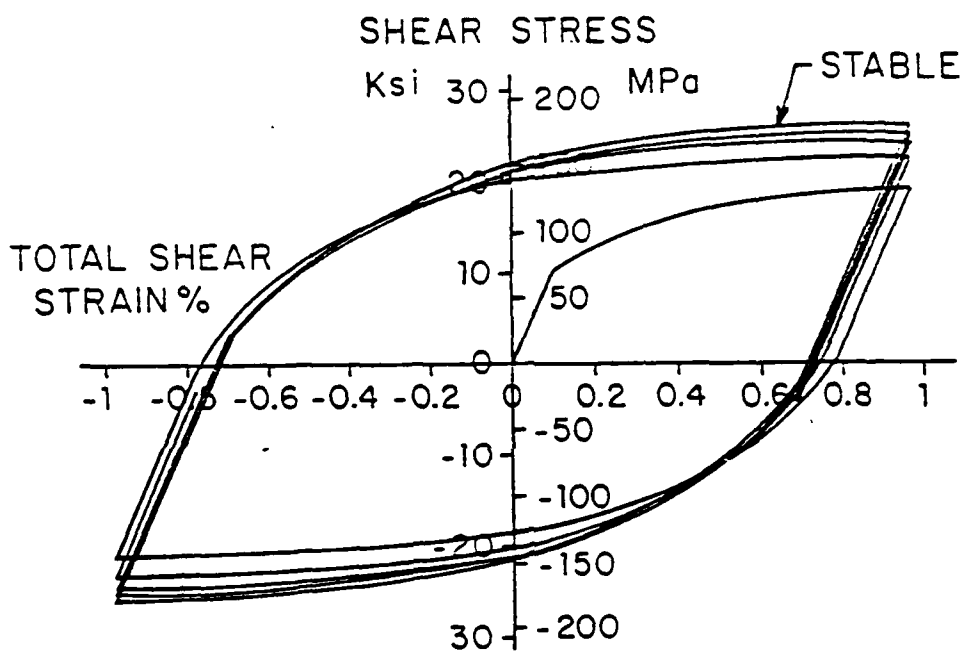


Figure 7. Theoretical shear stress-strain behavior of a hypothetical material.

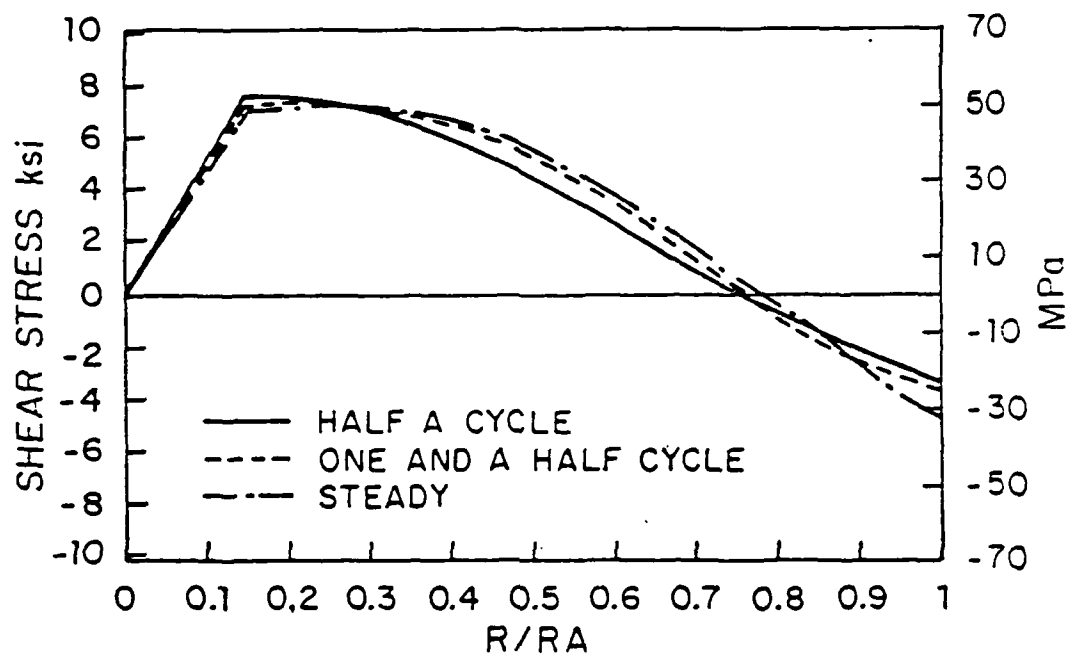


Figure 8. Residual stress distribution in a solid cylinder (hypothetical material) under cyclic torsion.

TECHNICAL REPORT INTERNAL DISTRIBUTION LIST

	<u>NO. OF COPIES</u>
CHIEF, DEVELOPMENT ENGINEERING BRANCH	
ATTN: SMCAR-LCB-D	1
-DA	1
-DP	1
-DR	1
-DS (SYSTEMS)	1
-DS (ICAS GROUP)	1
-DC	1
CHIEF, ENGINEERING SUPPORT BRANCH	
ATTN: SMCAR-LCB-S	1
-SE	1
CHIEF, RESEARCH BRANCH	
ATTN: SMCAR-LCB-R	2
-R (ELLEN FOGARTY)	1
-RA	1
-RM	2
-RP	1
-RT	1
TECHNICAL LIBRARY	5
ATTN: SMCAR-LCB-TL	
TECHNICAL PUBLICATIONS & EDITING UNIT	
ATTN: SMCAR-LCB-TL	2
DIRECTOR, OPERATIONS DIRECTORATE	1
DIRECTOR, PROCUREMENT DIRECTORATE	1
DIRECTOR, PRODUCT ASSURANCE DIRECTORATE	1

NOTE: PLEASE NOTIFY DIRECTOR, BENET WEAPONS LABORATORY, ATTN: SMCAR-LCB-TL, OF ANY ADDRESS CHANGES.

TECHNICAL REPORT EXTERNAL DISTRIBUTION LIST

<u>NO. OF COPIES</u>	<u>NO. OF COPIES</u>		
ASST SEC OF THE ARMY RESEARCH & DEVELOPMENT ATTN: DEP FOR SCI & TECH THE PENTAGON WASHINGTON, D.C. 20315	1	COMMANDER US ARMY AMCCOM ATTN: SMCAR-ESP-L ROCK ISLAND, IL 61299	1
COMMANDER DEFENSE TECHNICAL INFO CENTER ATTN: DTIC-DDA CAMERON STATION ALEXANDRIA, VA 22314	12	COMMANDER ROCK ISLAND ARSENAL ATTN: SMCR-ENM (MAT SCI DIV) ROCK ISLAND, IL 61299	1
COMMANDER US ARMY MAT DEV & READ COMD ATTN: DRCDE-SG 5001 EISENHOWER AVE ALEXANDRIA, VA 22333	1	DIRECTOR US ARMY INDUSTRIAL BASE ENG ACTV ATTN: DRXIB-M ROCK ISLAND, IL 61299	1
COMMANDER ARMAMENT RES & DEV CTR US ARMY AMCCOM ATTN: SMCAR-LC	1	COMMANDER US ARMY TANK-AUTMV R&D COMD ATTN: TECH LIB - DRSTA-TSL WARREN, MI 48090	1
SMCAR-LCE	1	COMMANDER	
SMCAR-LCM (BLDG 321)	1	US ARMY TANK-AUTMV COMD	
SMCAR-LCS	1	ATTN: DRSTA-RC	
SMCAR-LCU	1	WARREN, MI 48090	
SMCAR-LCW	1	COMMANDER	
SMCAR-SCM-O (PLASTICS TECH EVAL CTR, BLDG. 351N)	1	US MILITARY ACADEMY	
SMCAR-TSS (STINFO)	2	ATTN: CHMN, MECH ENGR DEPT	
DOVER, NJ 07801		WEST POINT, NY 10996	1
DIRECTOR BALLISTICS RESEARCH LABORATORY ATTN: AMXBR-TSB-S (STINFO) ABERDEEN PROVING GROUND, MD 21005	1	US ARMY MISSILE COMD REDSTONE SCIENTIFIC INFO CTR	
MATERIEL SYSTEMS ANALYSIS ACTV ATTN: DRXSY-MP ABERDEEN PROVING GROUND, MD 21005	1	ATTN: DOCUMENTS SECT, BLDG. 4484 REDSTONE ARSENAL, AL 35898	2
		COMMANDER	
		US ARMY FGN SCIENCE & TECH CTR	
		ATTN: DRXST-SD	
		220 7TH STREET, N.E.	
		CHARLOTTESVILLE, VA 22901	

NOTE: PLEASE NOTIFY COMMANDER, ARMAMENT RESEARCH AND DEVELOPMENT CENTER,
US ARMY AMCCOM, ATTN: BENET WEAPONS LABORATORY, SMCAR-LCB-TL,
WATERVLIET, NY 12189, OF ANY ADDRESS CHANGES.

TECHNICAL REPORT EXTERNAL DISTRIBUTION LIST (CONT'D)

<u>NO. OF COPIES</u>	<u>NO. OF COPIES</u>		
COMMANDER US ARMY MATERIALS & MECHANICS RESEARCH CENTER ATTN: TECH LIB - DRXMR-PL WATERTOWN, MA 01272	2	DIRECTOR US NAVAL RESEARCH LAB ATTN: DIR, MECH DIV CODE 26-27, (DOC LIB) WASHINGTON, D.C. 20375	1
COMMANDER US ARMY RESEARCH OFFICE ATTN: CHIEF, IPO P.O. BOX 12211 RESEARCH TRIANGLE PARK, NC 27709	1	COMMANDER AIR FORCE ARMAMENT LABORATORY ATTN: AFATL/DLJ AFATL/DLJG EGLIN AFB, FL 32542	1
COMMANDER US ARMY HARRY DIAMOND LAB ATTN: TECH LIB 2800 POWDER MILL ROAD ADELPHIA, MD 20783	1	METALS & CERAMICS INFO CTR BATTELLE COLUMBUS LAB 505 KING AVENUE COLUMBUS, OH 43201	1
COMMANDER NAVAL SURFACE WEAPONS CTR ATTN: TECHNICAL LIBRARY CODE X212 DAHLGREN, VA 22448	1		

NOTE: PLEASE NOTIFY COMMANDER, ARMAMENT RESEARCH AND DEVELOPMENT CENTER,
US ARMY AMCCOM, ATTN: BENET WEAPONS LABORATORY, SMCAR-LCB-TL,
WATERVLIET, NY 12189, OF ANY ADDRESS CHANGES.

END

FILMED

5-85

DTIC